Drug Development and Industrial Pharmacy, 23(4), 379-385 (1997)

RESEARCH PAPER

Dissolution Behavior of Oxazepam in Presence of Cyclodextrins: Evaluation of Oxazepam—Dimeb Binary System

J. R. Moyano, M. J. Arias, J. M. Ginés, J. I. Pérez, and A. M. Rabasco

Department of Pharmacy and Pharmaceutical Technology, Faculty of Pharmacy, University of Seville, 41012 Seville, Spain

ABSTRACT

The inclusion complex formation between oxazepam (Ox) and heptakis (2,6-di-O-methyl)-β-cyclodextrin (DIMEB) was studied in solution by solubility and ultraviolet spectroscopy methods, and in the solid state by differential scanning calorimetry, scanning electron microscopy, and powder x-ray diffractometry. The apparent stability constant, K_c, calculated by solubility and spectral data, was estimated as 642 and 588 M^{-1}, respectively. The solid complexes have been prepared by kneading and spray-drying techniques. The dissolution rate studies reveal that the better dissolution behavior corresponded to the spray-dried systems.

INTRODUCTION

Many investigations have been conducted on inclusions in cyclodextrins (CDs) and their derivatives, in order to improve the stability and/or solubility and bioavailability of different pharmaceutically active ingredients (1,2).

Recently, the chemically modified CDs have become more interesting because their physicochemical properties and inclusion behavior are different from those of the natural CDs. Most of the CD derivatives are highly water soluble and can therefore provide a greater increase in the water solubility of the guest molecules than natural CDs. Methyl CDs were, among the first CD derivatives, the most intensively studied from a pharmaceutical view point (3). Among them, the most useful is the heptakis-(2,6-di-*O*-methyl)-β-cyclodextrin (DIMEB) (4). This derivative is extremely soluble in water and interacts with a wide variety of drug molecules (5–9).

Oxazepam (Ox) is a 3-hydroxybenzodiazepine frequently applied in therapy against anxiety and as anticonvulsive, sedative, and hypnotic, specially for older and alcoholic patients. However, it has a poor water solubility and dissolution rate, whereas its pharmacological action requires a rapid plasma appearance. Over recent years it has become clear that the absorption rate of 3-hydroxybenzodiazepines from the gut after oral administration is formulation dependent (10). These

characteristics make Ox a suitable candidate for inclusion complexation in CDs.

The inclusion behavior in the liquid medium and in the solid state of Ox–DIMEB system has been studied by phase solubility diagrams, spectral shift method, x-ray diffractometry (XRD), differential scanning calorimetry (DSC), and scanning electron microscopy (SEM). In addition, other studies have been also carried out to evaluate the different techniques for preparing a solid complex of Ox with DIMEB for potential use in the development of a suitable oral formulation.

MATERIALS AND METHODS

Ox (Boehringer-Ingelheim, E-Barcelona) and DIMEB (Cyclolab, H-Budapest) of commercial purity grade were used. All other materials were of analytical reagent grade.

Phase Solubility Studies

Solubility measurements were performed according to Ref. 11. Excess amounts of Ox were added to Erlenmeyer flasks containing aqueous solutions of DIMEB at various concentrations (0.02–0.1 M). These flasks were shaken at room temperature for approximately 1 week. The suspensions were filtered, properly diluted, and assayed for drug concentration by ultraviolet spectroscopy (UV) at 230 nm.

Ultraviolet Spectroscopy

UV spectra of $1.8 \cdot 10^{-6}$ M Ox with increasing concentrations of DIMEB were recorded on a Hitachi U-2000 UV–VIS spectrophotometer. The absorbance change of the substrate (Ox) was measured at 230 nm.

Preparation of Solid Complexes

Kneading Method

The CD was put in a mortar, wetted with purified water, and kneaded. The Ox was added and the mixture was then kneaded (45 min). The final product was dried at 37°C for 48 hr, pulverized, and sieved (50–250 μm).

Spray-Drying Method

Ox and DIMEB were dissolved in 400 ml of 96% ethanol and in 400 ml of purified water, respectively. The solutions were further mixed and spray dried (Büchi 190M miniSpray-Dryer). Conditions were: flow rate: 1000 ml/hr, inlet temperature: 165°C, outlet temperature: 95°C, air flow rate: 500 nl/hr^{-1}.

Differential Scanning Calorimetry

The samples was analyzed by DSC using a Mettler FP85 furnace, a FP80 HT temperature control unit, and FP89 HT software. The samples (10 mg) were put into pierced aluminum pans. The studies were performed under static air atmosphere in the temperature range of 100° to 320°C, at a heating rate of 10°C/min.

Scanning Electron Microscopy

The morphological features of the Ox–DIMEB systems (physical mixture, kneaded and spray dried) were analyzed by SEM (Philips XL30), employing a 20-kV tension.

X-ray Diffractometry Studies

The x-ray diffractograms were carried out using x-ray diffraction equipment (Siemens Kristallofex D-500), with Ni-filtered CuK_α radiation, voltage 36 kV and current 26 mA. The scanning speed was 1° (2θ)/min, the chart speed 1 cm/min, and the adequate sensibility was commonly $2 \cdot 10^4$ cps.

Dissolution Rate Studies

The dissolution studies of different samples were performed according to USP XXII, by the rotating basket method (Turu Grau, Model D-6). The samples were placed into hard gelatin capsules. USP XXII artificial gastric medium, 1000 ml, without enzymes were employed as dissolution medium, at a temperature of 37° ± 0.5°C. The stirring speed was 50 rpm. The aliquots were withdrawn at various time intervals and analyzed spectrophotometrically. All assays were run in triplicate.

RESULTS AND DISCUSSION

Phase Solubility Studies

The phase solubility diagram for the Ox–DIMEB system in water at 20°C is shown in Fig. 1. The solubility of Ox enlarges linearly with increasing concentrations of DIMEB, showing thus a typical A_L-type phase solubility curve. This curve may be ascribed to the formation of a stoichiometric 1:1 complex. Consequently, solid complexes could not be prepared by

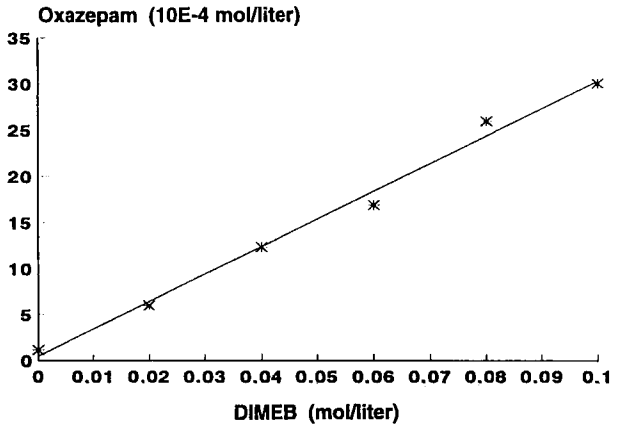

Figure 1. Solubility of Ox in water at 20°C as a function of DIMEB concentration.

coprecipitation, a method that is applied only for systems showing B_S-type phase solubility diagram. For this reason, in our case, we must apply other elaboration methods. The selected ones for this study were the kneading and the spray-drying techniques.

The apparent 1:1 stability constant K_c was calculated from the straight line of the phase solubility diagram by means of the following equation:

$$K_c = \frac{\text{slope}}{\text{intercept}\,(1-\text{slope})}$$

The constant value was 642 M^{-1}, a large value compared with those obtained with the β-CD, 2-hydroxypropyl-β-CD (HP-β-CD), and γ-CD in previous works (12–14) (Table 1). This fact may be attributed to the flexible structure of DIMEB, where any possibility exists of intramolecular hydrogen bonds between the *O*-methylated hydroxyl groups of C_2 or C_6 glucopyranose units in contrast with β-CD. Hence, we can see how flexible conformations are very favorable to the adaptation of Ox into the cavity of the CD molecule.
In the case of γ-CD, when comparing, we can appreciate how the cavity size of DIMEB appears to be more convenient for the accommodation of Ox molecule, in respect to the too-large cavity of γ-CD.

Table 1

Apparent Stability Constant Values for the Different Ox–CD Systems

CD	DIMEB	β-CD	HP-β-CD	γ-CD
K_c (M^{-1})	642	205	145	41

Moreover, it can be predicted that the cavity of DIMEB mainly entraps the phenyl group of the Ox molecule. This estimation is in good agreement with the values obtained for similar molecules by other authors (15).

UV Studies

Ox solution UV spectra at increasing DIMEB concentrations were studied. An example is shown in Fig. 2. From these spectra, it arises that Ox λ_{max} peak at 230 nm showed a bathochromic shift, with an intensity absorption decrease in presence of DIMEB. This phenomenon may be assigned to a complex formation. As is well known, the UV spectra shifts are attributed to a partial shielding of the excitable drug electrons into the CD cavity (16).

Because the complex and drug molar absorptivities differed at the same wavelength, it was possible to determine the stability constant from these spectral data by the double reciprocal plot method (17). This plot representing $1/\Delta A$ versus $1/[CD]$ was linear (Fig. 3), indicating the presence of a 1:1 complex.

The apparent 1:1 stability constant (K_c) was determined by the Benesi–Hildebrand equation (18):

$$\frac{1}{\Delta A} = \frac{1}{[D]\,K_c \Delta\varepsilon}\frac{1}{[CD]} + \frac{1}{[D]\,\Delta\varepsilon}$$

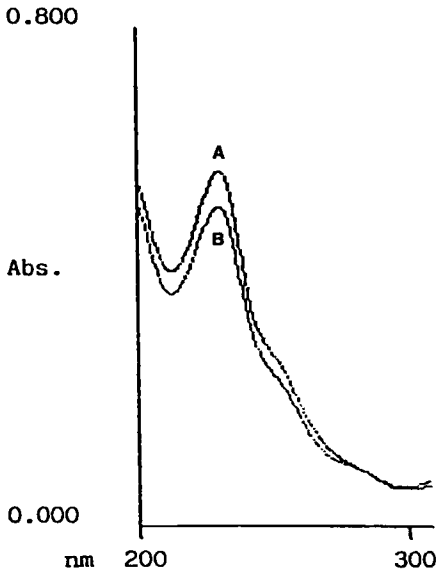

Figure 2. Effect of DIMEB concentration on UV absorption spectra of Ox in water. Drug concentration: $1.85 \cdot 10^{-6}$ M; DIMEB concentration: curve A = 0, curve B = $1.6 \cdot 10^{-3}$ M.

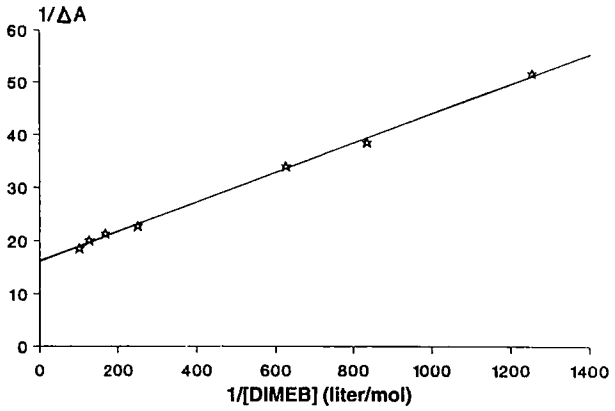

Figure 3. Benesi–Hildebrand plot for the effect of DIMEB on the Ox absorbance at $\lambda = 230$ nm.

where ΔA is the difference of absorbance at 230 nm, $[CD]$ is the CD concentration, $[D]$ is the drug concentration (constant), and $\Delta\varepsilon$ are the molar absorptivities difference between the complex and the free drug.

The stability constant K_c was obtained from the intercept/slope ratio. The value obtained was 588 M^{-1}, a datum that is in good agreement with that obtained from phase solubility studies. Moreover, this K_c value is included in the range of 200 and 5000 M^{-1}, considered by various authors as the most suitable, given that, in this range, the formation of an inclusion complex may contribute to the improvement of bioavailability of poorly soluble drugs (19).

Thermal Characterization

Thermal traces of the samples under study are reported in Fig. 4. The Ox thermogram [Fig. 4(I)] displays its endothermic melting peak at 215°C and a broad exothermal effect in the range of 300°C, related to the beginning of the drug decomposition. The thermogram of the spray-dried DIMEB [Fig. 4(B)] shows an exothermic peak at 185°C, which may be ascribed to the crystallization of the amorphous DIMEB (20). The DSC curves of the binary systems [Figs. 4(C) to 4(H)] exhibited the persistence of the Ox endotherm but did not show the exothermic effects of the crystallization of DIMEB and the decomposition of the pure Ox, except the spray-dried systems [Figs. 4(G) and 4(H)]. These show an exothermic effect at 128°C, which may be attributed to the crystallization of the inclusion complex (21). The evaluation of the DSC traces demonstrated that the Ox melting heat involved in the process was different in the three systems (Table 1). In the case

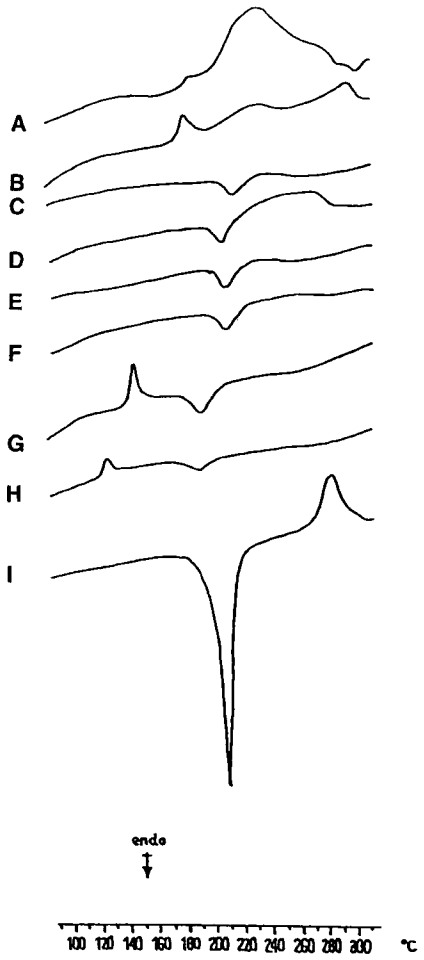

Figure 4. DSC thermograms for the Ox–DIMEB products: A, pure DIMEB; B, spray-dried DIMEB; C, 1:1 physical mixture; D, 1:2 physical mixture; E, 1:1 kneaded mixture; F, 1:2 kneaded mixture; G, 1:1 spray-dried system; H, 1:2 spray-dried system; I, pure Ox.

of the spray-dried products, the endotherm is slightly shifted to low temperatures and strongly reduced in its intensity, denoting thus the drug complexation. Finally, we have calculated the average percentages of complexed Ox from DSC integration peak data (Table 2), based on the assumption of the dependence between both parameters, by the following expression:

$$\%\ \text{complexed} = \frac{\Delta H_{f\,PM} - \Delta H_{fx}}{\Delta H_{f\,PM}} \times 100$$

where $\Delta H_{f\,PM}$ is the fusion enthalpy value corresponding to the Ox endotherm in the physical mixture, and

Table 2

Evaluation of Thermodynamic Parameters

Sample	T_0 (°C)	T_P (°C)	ΔH_f (J/g)
PM 1:1	200.7	211.2	-37.2
KM 1:1	184.0	205.7	-30.2
SD 1:1	172.7	185.4	-26.5
PM 1:2	194.8	204.4	-25.0
KM 1:2	191.6	206.2	-20.6
SD 1:2	174.9	187.4	-11.9
Ox	197.3	215.3	-253.0

Note. T_0: initial melting temperature, T_P: peak fusion temperature, ΔH_f: enthalpy of fusion, by DSC for Ox and the different Ox-DIMEB systems; PM: physical mixture, KM: kneaded mixture, SD: spray-dried powder.

ΔH_{fX} is the enthalpy value for the kneaded or the spray-dried systems. The results obtained are summarized in Table 3.

From these data it can be deduced that the spray-drying technique provides a major complexation yield with respect to the kneaded products. On the other hand, it is clear that the DIMEB ratio has an influence in the spray-dried products but not in the kneading outputs. These facts can be explained on the basis of a major interaction between Ox and DIMEB for the spray-dried technique, in contrast with kneading. This affirmation is reinforced by the results obtained by phase solubility studies.

SEM Analysis

The Ox-DIMEB systems micrographs are reported in Figs. 5 to 7. Whereas the physical mixture showed the crystalline structure of Ox and DIMEB, the features of both crystals in the kneaded mixture were not easily detectable. Furthermore, the micrograph of the spray-dried system showed an amorphous product, with the presence of small-size particles tending to aggregation. This observation led us to estimate the existence of a

Table 3

Average Complexation Percentages Calculated from ΔH_f Values for the Kneaded (KM) and Spray-Dried (SD) Ox-DIMEB Systems

Sample	KM 1:1	SD 1:1	KM 1:2	SD 1:2
% complexed	19.4	28.8	17.6	52.4

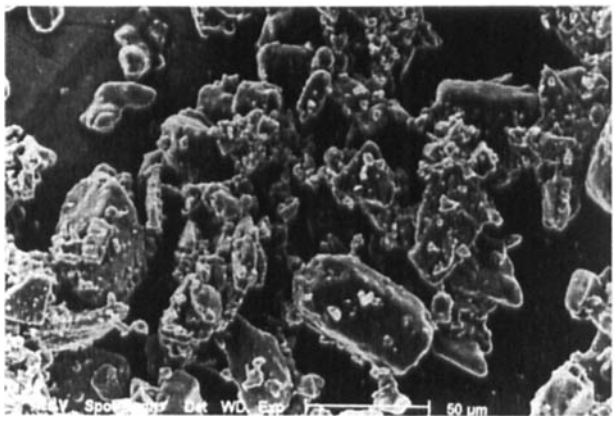

Figure 5. Ox-DIMEB physical mixture SEM micrograph.

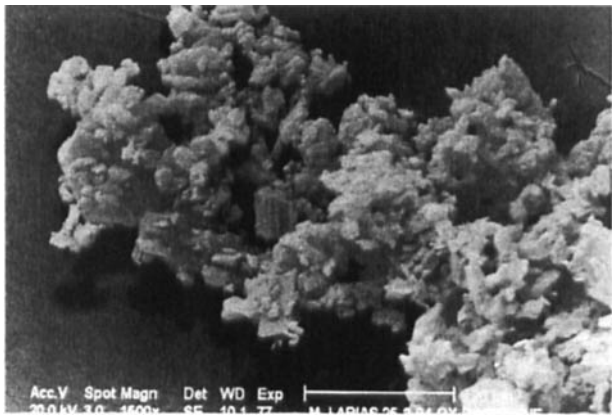

Figure 6. Ox-DIMEB kneaded mixture SEM micrograph.

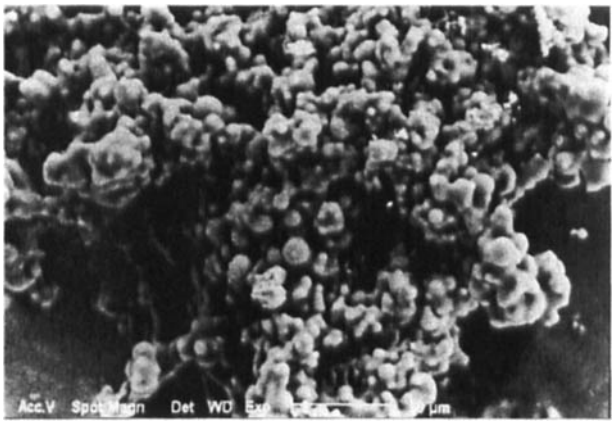

Figure 7. Ox-DIMEB spray-dried SEM micrograph.

single component in the obtained preparations. Similar observations were carried out by other authors (22).

In general, SEM morphology studies of Ox–CD systems helped us to explain the dissolution behavior of these systems by relating structure and particle size of the materials with their correspondent release profiles. This aspect was discussed earlier.

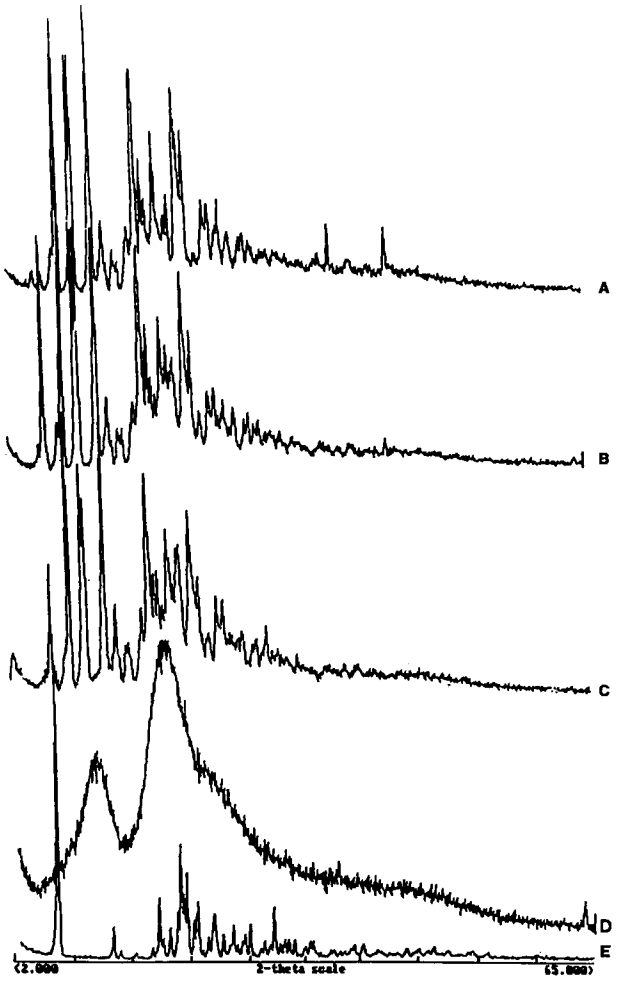

Figure 8. X-ray diffractograms for the following products: A, DIMEB; B, 1:1 physical mixture; C, 1:1 kneaded mixture; D, 1:1 spray-dried product; E, pure Ox.

XRD Records

The XRD patterns of the raw materials and binary systems are shown in Fig. 8. While x-ray diffractograms for the physical mixture and the kneaded system are superpositions of the two pure components, the spray-dried product shows a diffuse diffraction pattern, suggesting the lesser crystallinity of this formulation, confirmed by electron microscopy data.

It is clearly observed that the diffraction peaks of Ox at 6° and 30° (2θ) for this system disappear, in contrast with the persistence of these peaks for the pure Ox spray dried. This fact may be attributed to an interaction between Ox and DIMEB, showing the presence of a new solid phase, where a possible formation of a inclusion complex was contemplated. These observations are in concordance with the results of the DSC studies.

Dissolution Rate Studies

The dissolution profiles were evaluated by means of the dissolution efficiency parameter over the first 15 and 60 min (DE_{15} and DE_{60}, respectively) (23) and the dissolution percentage over the first 30 min (DP_{30}) (Table 4).

From these data, we can remark how the spray-dried systems' dissolution rates were extremely large compared with those of the free drug and the physical mixtures, which only exhibited a slight improvement in reference to free Ox. This fact is in good agreement with the DSC and XRD studies and related with the reduction of the crystallinity of the system (24) and the important role played by the complexation process. The influence of CD ratio on the dissolution profiles of spray-dried preparations was not significant. It is due to the large enhancement of dissolution rate from the 1:1 system, which cannot be improved by the increase of the DIMEB proportion.

Table 4

In Vitro Dissolution Parameters for the Indicated Systems

Systems	PM 1:1	KM 1:1	SD 1:1	PM 1:2	KM 1:2	SD 1:2	Ox
DP_{30}	37.93	35.00	88.40	42.42	54.62	92.65	27.42
DE_{15}	0.1299	0.1572	0.5982	0.1350	0.2124	0.6158	0.0870
DE_{60}	0.3418	0.3125	0.8179	0.3710	0.4819	0.8591	0.2211

Note. PM: physical mixture; KM: kneaded mixture; SD: spray-dried powder.

The kneaded systems also exhibited a good improvement of the dissolution rate of Ox. In this case, the 1:2 kneaded mixture exhibited a faster dissolution rate than the 1:1 kneaded mixture. This conduct may be attributed to the hydrophilic DIMEB wetting effect, which is more pronounced for the kneaded systems than for the physical mixtures. This fact is assigned to the major interaction between Ox and CD in the case of the kneaded products.

REFERENCES

1. D. Duchêne and D. Wouessidjewe, Drug Dev. Ind. Pharm., 16, 2487 (1990).
2. O. Bekers, E. V. Uijtendaal, J. H. Beijnen, A. Bult, and W. J. M. Underberg, Drug Dev. Ind. Pharm., 17, 1503 (1991).
3. D. Duchêne and D. Wouessidjewe, Pharm. Tech. Int., 2, 21 (1990).
4. J. Szejtli, Starch/Stärke, 36, 429 (1984).
5. N. Celebi and T. Nagai, Drug Dev. Ind. Pharm., 14, 63 (1988).
6. Y. Nakai, K. Yamamoto, T. Oguchi, E. Yonemochi, and T. Hanawa, Chem. Pharm. Bull., 38, 1345 (1990).
7. M. O. Ahmed, Y. Nakai, A. E. S. Aboutaleb, K. Yamamoto, A. A. Z. A. Rahman, and S. I. Saleh, Chem. Pharm. Bull., 38, 3423 (1990).
8. F. W. H. M. Merkus, J. C. Verhoef, S. G. Romeijn, and N. G. M. Schipperly, Pharm. Res., 8, 588 (1991).
9. R. J. Prankerd, H. W. Stone, K. B. Sloan, and J. H. Perrin, Int. J. Pharm., 88, 189 (1992).
10. M. E. Pickup, M. S. Rogers, and A. P. Launchbury, Int. J. Pharm., 22, 311 (1984).
11. T. Higuchi and K. A. Connors, Adv. Anal. Chem. Instr., 4, 117 (1965).
12. J. R. Moyano, J. M. Ginés, M. J. Arias, and A. M. Rabasco, Pharm. Acta Helv., 69, 81 (1994).
13. J. R. Moyano, J. M. Ginés, M. J. Arias, and A. M. Rabasco, Int. J. Pharm., 114, 95 (1995).
14. J. R. Moyano, M. J. Arias, J. M. Ginés, and A. M. Rabasco, Farmaco, 50, 791 (1995).
15. A. Yoshida, H. Arima, K. Uekama, and J. Pitha, Int. J. Pharm., 46, 217 (1988).
16. J. Szejtli, ed., *Cyclodextrins and Their Inclusion Complexes*, Academiai Kiado, Budapest, 1982, p. 177.
17. K. A. Connors and J. A. Mollica, J. Pharm. Sci., 55, 772 (1966).
18. H. A. Benesi and J. H. Hildebrand, J. Am. Chem. Soc., 71, 2703 (1949).
19. J. Blanco, J. L. Vila-Jato, F. Otero, and S. Anguiano, Drug Dev. Ind. Pharm., 17, 943 (1991).
20. A. A. A. Rahman, S. I. Saleh, Y. Nakai, A. E. Aboutaleb, and M. O. Ahmed, Eur. J Pharm. Biopharm., 39, 82 (1993).
21. G. A. El-Gendy and M. A. El-Gendy, Eur. J. Pharm. Biopharm., 39, 249 (1993).
22. S. S. Tous, STP Pharm., 6, 635 (1990).
23. K. A. Khan, J. Pharm. Pharmacol., 27, 48 (1975).
24. K. Uekama, K. Oh, M. Otagiri, H. Seo, and M. Tsuruoka, Pharm. Acta Helv., 58, 338 (1983).